Structural and electronic changes accompanying reduction of Cr(CO)₄(bpy) to its radical anion: a quantum chemical interpretation of spectroelectrochemical experiments

Stanislav Záliš,[a] Chantal Daniel[b] and Antonín Vlček, Jr. *[a,c]

[a] *J. Heyrovský Institute of Physical Chemistry, Academy of Sciences of the Czech Republic, Dolejškova 3, CZ-182 23 Prague, Czech Republic*
[b] *Laboratoire de Chimie Quantique, UMR 7551 du CNRS et de l'Université Louis Pasteur, 4, rue Blaise Pascal, Strasbourg, F-67008, France*
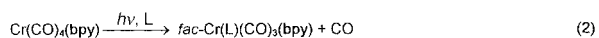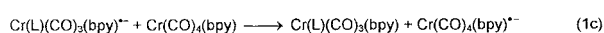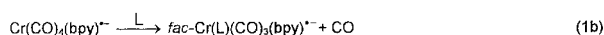[c] *Dept. of Chemistry, Queen Mary and Westfield College, Mile End Road, London, UK E1 4NS. E-mail: a.vlcek@qmw.ac.uk*

Optimised molecular structures and charge distributions within Cr(CO)₄(bpy) and its radical anion were calculated using density functional theory (DFT). It was found that, although reduction predominantly concerns the bpy ligand, its structural and electronic effects extend to the Cr(CO)₄ fragment. Each equatorial and axial CO ligand was calculated to accept 7.1 and 4.8%, respectively, of the extra electron density in Cr(CO)₄(bpy)$^{\cdot-}$. This is in accordance with the IR spectroelectrochemical results which show that the corresponding CO stretching force constants decrease by 68 and 21 N m^{-1}, respectively. The calculated spin density in Cr(CO)₄(bpy)$^{\cdot-}$ resides predominantly on the bpy ligand which behaves spectroscopically as bpy$^{\cdot-}$. The spin density is delocalised to both axial and equatorial pairs of CO ligands by mixing of π*(C≡O) orbitals with the, predominantly π*(bpy), SOMO. In addition, part of the spin density is delocalised selectively to the axial CO ligands by an admixture of their σ orbitals into the SOMO. This σ–π* contribution is responsible for isotropic EPR hyperfine splitting which was observed from the axial ^{13}C(CO) atoms only. Accordingly, the isotropic hyperfine splitting constants correlate with calculated Fermi contact terms instead of total spin densities. Complete active space self-consistent field (CASSCF)-calculated changes in charge distribution upon a Cr→bpy MLCT excitation show that the electron density localised on the bpy ligand increases by about the same amount upon reduction or MLCT-excitation of Cr(CO)₄(bpy). The axial CO ligands are depopulated by MLCT excitation *ca.* 1.6 times more than the equatorial ones. These conclusions can be generalised and applied to other coordination and organometallic complexes of low-valent metals which contain a reducible or radical-anionic ligand.

Introduction

The Cr(CO)₄(bpy) complex is widely studied as a prototype of an inert organometallic molecule which can be activated by an electron transfer or metal to ligand charge transfer (MLCT) excitation.[1–15] Both one-electron reduction and irradiation into the Cr→bpy MLCT absorption band labilise the axial Cr–CO bond, making the CO ligand susceptible to a facile substitution by a solvent molecule or by a Lewis base, L (*e.g.* phosphine) present in solution (Scheme 1).

Cr(CO)₄(bpy) $\xrightarrow{e^-}$ Cr(CO)₄(bpy)$^{\cdot-}$ (1a)

Cr(CO)₄(bpy)$^{\cdot-}$ $\xrightarrow{L}$ *fac*-Cr(L)(CO)₃(bpy)$^{\cdot-}$ + CO   (1b)

Cr(L)(CO)₃(bpy)$^{\cdot-}$ + Cr(CO)₄(bpy) $\longrightarrow$ Cr(L)(CO)₃(bpy) + Cr(CO)₄(bpy)$^{\cdot-}$ (1c)

Cr(CO)₄(bpy) $\xrightarrow{h\nu, L}$ *fac*-Cr(L)(CO)₃(bpy) + CO   (2)

Scheme 1

The reductive activation,[8] described by Scheme 1, eqn. 1(a)–(c), amounts to an electron transfer catalysed reaction since the radical-anionic product reacts with the starting molecule, regenerating the active Cr(CO)₄(bpy)$^{\cdot-}$ species [Scheme 1, eqn. 1(c)]. Both the reactive MLCT excited state and Cr(CO)₄(bpy)$^{\cdot-}$ involved in the photochemical and reductive activation, respectively, contain a coordinated bpy$^{\cdot-}$ radical anion. Hence, some specific interaction between the Cr(CO)₄ moiety and the singly occupied π* orbital of the bpy$^{\cdot-}$ ligand

can be suspected of labilising the axial Cr–CO bonds of Cr(CO)₄(bpy). However, the analogy[16] between reduction and MLCT excitation has obvious limitations manifested by the fact that photochemical CO dissociation is an ultrafast process occurring in <400 fs while the Cr(CO)₄(bpy)$^{\cdot-}$ radical anion reacts on a time scale of minutes.[7,8]

Recently, we have studied the localisation of the extra electron in Cr(CO)₄(bpy)$^{\cdot-}$ by a combination of IR and EPR spectroelectrochemistry[9] while the MLCT excitation was investigated by resonance Raman spectroscopy.[10] Spectroelectrochemical studies took advantage of a ^{13}CO isotopic enrichment which allowed us to determine the EPR hyperfine interaction with the C atoms of the CO ligands and the changes in the force constants of the stretching vibrations of axial and equatorial CO ligands. EPR spectra of Cr(CO)₄(bpy)$^{\cdot-}$ and its ^{13}CO-enriched isotopomers have shown that the extra electron is predominantly localised on the bpy$^{\cdot-}$ ligand. Importantly, a hyperfine interaction was found to occur only with the axial ^{13}C atoms, the equatorial ones being EPR silent. Simple-minded interpretation of this observation would indicate much larger spin density on the axial than equatorial CO ligands. Seemingly in contradiction, reduction of Cr(CO)₄(bpy) causes the stretching force constant of the equatorial CO ligands to decrease about three times more than that of the axial CO's, suggesting that the π-back donation to the equatorial CO ligands of the Cr(CO)₄(bpy)$^{\cdot-}$ radical anion is much stronger than to the axial ones. Experimental results thus demonstrated that the reduction of the bpy ligand in Cr(CO)₄(bpy) has a

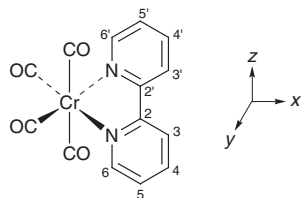**Fig. 1** The Cr(CO)$_4$(bpy) molecule and chosen orientation of axes.

profound influence on the bonding within the Cr(CO)$_4$ fragment. At the same time, the IR and EPR data showed that the axial and equatorial CO ligands are affected by very different mechanisms.

Herein, we report results of DFT calculations of the electronic and molecular structure of Cr(CO)$_4$(bpy), and its radical anion, which reveal how bpy-localised reduction affects the electron density distribution and bonding within the Cr(CO)$_4$ moiety. Moreover, a comparison of these results with the CASSCF wave function of the d$_{xz}$→π*(bpy) ^{1}bA$_1$ MLCT excited state[6,11] is used to compare the electronic effects of reduction and MLCT excitation. Using Cr(CO)$_4$(bpy) as a prototypical example, this study addresses more general questions of the localisation of redox changes in complexes containing redox-active ligands, the role of 'spectator' ligands, and relations between the extent of ligand reduction caused by electron addition or MLCT excitation. It has been found that neither the reduction nor MLCT excitation can be regarded as localised solely on the acceptor ligand or the metal–ligand moieties, respectively, since the bonding within the remaining part of the coordination sphere is strongly affected as well.

Calculations

Gaussian 98[17] and MOLCAS[18] program packages were used for DFT and CASSCF calculations, respectively. Density functional theory (DFT) was employed to calculate the ground state electronic structure of Cr(CO)$_4$(bpy) and its radical anion. DFT calculations of the latter were spin unrestricted. Calculations were performed within the constraint of C_{2v} symmetry, the bpy ligand being located in the xy plane, with the C_2 symmetry axis coincident with the x axis (Fig. 1).

B3LYP hybrid functionals[19] were used. Cr valence double-ζ plus polarisation basis set designed for DFT calculations was taken from Godbout et al.[20] Dunning's[21] valence double-ζ with polarisation functions were used for C, N and H atoms (= basis set I) for geometry optimisation, calculations of charge density and spin distribution, and Fermi contact terms. Isotropic hyperfine coupling constants were calculated at the optimised geometry. In order to describe the effect of basis variation on the spin density distribution and Fermi terms, several different basis sets were used for C, N and H atoms within single point calculations: double-ζ wave functions with polarisation functions of Adamo and Barone[22] designed for EPR calculations (EPR-II basis, = basis set II), and 6-311G++**[23,24] (= basis set III).

The description of lowest excited states of Cr(CO)$_4$(bpy) is based on CASSCF calculations. Here, the generally contracted atomic natural orbital (ANO) type basis sets were used: for the first-row atoms a (10,6) contracted to (3,2), and for hydrogen atoms a (7) set contracted to (2). These calculations were performed using an idealised molecular geometry taken from ref. 15.

Results

Molecular geometry

Calculated important bond lengths and angles of Cr(CO)$_4$(bpy) and its reduced form are summarised in Table 1. The reduction affects mainly the geometry of the bpy ligand. The lengthening

Table 1 Selected DFT calculated bond lengths (Å) and angles (°) of Cr(CO)$_4$(bpy) and its radical anion

	Cr(CO)$_4$(bpy)	Cr(CO)$_4$(bpy)$^{\cdot-}$	Change on reduction
Cr–N	2.127	2.147	+0.020
Cr–C$_{ax}$	1.915	1.909	−0.006
Cr–C$_{eq}$	1.861	1.847	−0.014
N1–C2	1.361	1.394	+0.033
C2–C3	1.404	1.431	+0.025
C3–C4	1.394	1.380	−0.014
C4–C5	1.401	1.423	+0.022
C5–C6	1.394	1.396	+0.002
C6–N1	1.350	1.342	−0.008
C2–C2′	1.476	1.427	−0.049
(C–O)$_{ax}$	1.163	1.168	+0.005
(C–O)$_{eq}$	1.170	1.179	+0.009
Cr–N1–C2	117.5	115.6	−1.9
Cr–N1–C6	124.6	126.0	+1.4
N1–C2–C2′	114.6	116.1	+1.5
C$_{ax}$–Cr–C$_{ax}$	173.6	176.5	+2.9
C$_{eq}$–Cr–C$_{eq}$	93.1	92.6	−0.5
N–Cr–N	75.7	76.4	+0.7

Table 2 Calculated charges (e) on subsystems of Cr(CO)$_4$(bpy) and its radical anion

	Cr(CO)$_4$(bpy)	Cr(CO)$_4$(bpy)$^{\cdot-}$	Change on reduction
Cr	−0.043	−0.051	−0.008
bpy	0.263	−0.493	−0.756
(CO)$_{ax}$	−0.012	−0.061	−0.048[a]
(CO)$_{eq}$	−0.098	−0.169	−0.071[b]

[a] Out of this, the charge on the O atom changes by −0.046. [b] Out of this, the charge on the O atom changes by −0.056.

of the N1–C2 and shortening of the C2–C2′ bonds are the most significant changes. The Cr–N bonds are elongated. To a lesser extent, reduction also influences the calculated structure of the Cr(CO)$_4$ moiety. Addition of an electron is accompanied by contraction of Cr–CO bonds and elongation of C–O bonds. Bond length changes within the equatorial Cr(CO)$_2$ fragment are about twice as large as those in the axial OC–Cr–CO moiety.

Charge distribution

Table 2 summarises calculated charges on the Cr atom, bpy, axial and equatorial CO ligands in Cr(CO)$_4$(bpy) and its radical anion. It follows that the extra electron density in the latter is mostly localised on the bpy ligand. However, a significant charge delocalisation to the CO ligands occurs. The equatorial CO ligands are better electron acceptors than the axial ones in both the neutral and anionic forms of Cr(CO)$_4$(bpy), as is manifested by much larger negative charges. Upon reduction, the equatorial pair of CO ligands accepts about 14.2% of the extra electron density in the radical anion while the two axial CO ligands accommodate only 9.6% (Table 2). The charge on the Cr atom is virtually unchanged by the reduction.

The change in the charge distribution in Cr(CO)$_4$(bpy) upon vertical excitation to the b^{1}A$_1$ MLCT excited state,[6] which originates predominantly in a d$_{xz}$→π*(bpy) excitation, was calculated at a CASSCF level and results are summarised in Table 3. The MLCT excitation increases the electron density at the bpy ligand by 79% cf. a value of 76% (Table 2) calculated for the reduction.

Molecular orbitals

DFT-calculated one-electron orbital energies of Cr(CO)$_4$(bpy) and its radical anion are qualitatively depicted in Fig. 2. The

Table 3 The CASSCF-calculated charge distribution in the ground state and b^1A_1 MLCT excited state of $Cr(CO)_4(bpy)$. Calculations were performed with 10 correlated electrons in 11 active orbitals

	G.S.	E.S.	Difference
Cr	0.062	0.419	0.357
bpy	0.219	−0.570	−0.789
$(CO)_{ax}$	−0.001	0.132	0.131
$(CO)_{eq}$	−0.139	−0.057	0.082

Table 4 Calculated contributions (%) of subsystems of $Cr(CO)_4(bpy)$ and its radical anion to the redox orbital, *i.e.* the LUMO and SOMO, respectively

	$Cr(CO)_4(bpy)$	$Cr(CO)_4(bpy)^{\cdot-}$	Change on reduction
Cr	2.52	1.94	−0.58
bpy	92.14	93.74	+1.60
$(CO)_{ax}$	1.69	1.40[a]	−0.29
$(CO)_{eq}$	0.98	0.79[b]	−0.19

[a] The σ component accounts for 0.86%, with a 0.84% participation of the $2p_z$ and 2s orbitals at each C atom. The π component accounts for 0.54% with a 0.32% participation of the C $2p_x$ orbital. [b] π-Component only. The C $2p_z$ orbital contributes by 0.43%.

Fig. 2 Qualitative MO schemes of the $Cr(CO)_4(bpy)$ (left) and $Cr(CO)_4(bpy)^{\cdot-}$ (right) complexes based on DFT calculations. The HOMOs of the neutral and anionic complexes are set at the same energy value.
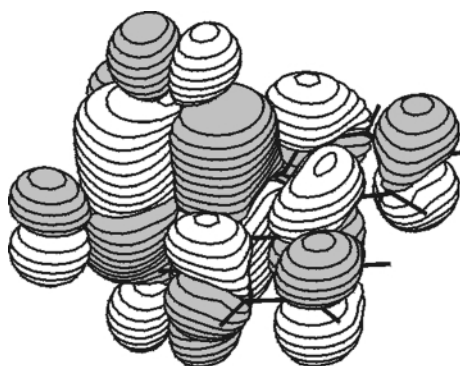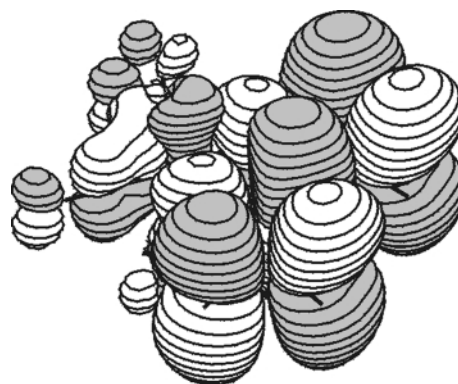

Fig. 3 The composition of the b_2 HOMO orbital of $Cr(CO)_4(bpy)$.

Fig. 4 The composition of the b_2 SOMO orbital of $Cr(CO)_4(bpy)^{\cdot-}$. The σ-contribution to the SOMO is clearly visible along the axial Cr–CO bond.

a_1, a_2 and b_2 set of the highest occupied molecular orbitals (HOMOs) of both the neutral and anionic species have a large contribution from the Cr $d_{x^2-y^2}$, d_{xy} and d_{xz} orbitals, respectively. The b_2 HOMO orbital is shown in Fig. 3. It has *ca.* 50% d_{xz} character in both species. The bpy ligand in the neutral and anionic species contributes by 23.5 and 21%, respectively. Each axial and equatorial CO ligand contributes to the b_2 HOMO of $Cr(CO)_4(bpy)$ by 8.75 and 4.20%, respectively. These contributions increase to 9.65 and 5.01%, respectively, upon reduction. For symmetry reasons, the equatorial CO ligands contribute to the b_2 HOMO only by their $\pi^*(p_z)$ orbitals. The axial CO ligands participate in the b_2 HOMO by both their $\pi^*(p_x)$ and σ(s, p_z) orbitals. The π contribution predominates. It amounts to 8.09 and 8.41% per axial CO in the neutral and anionic species, respectively. The σ-contribution per axial CO increases from 0.66 to 1.24% on going from $Cr(CO)_4(bpy)$ to the radical anion. (Note that the out-of-phase combination of σ orbitals of the two axial CO ligands, $\sigma_1 - \sigma_2$, belongs to the same b_2 symmetry representation of the C_{2v} point group of the $Cr(CO)_4(bpy)$ molecule as the lowest $\pi^*(bpy)$ orbital, allowing for a σ–π^* mixing in both HOMO and LUMO.)

The b_2 lowest lying molecular orbital (LUMO) of $Cr(CO)_4(bpy)$ is half-filled during the reduction process, becoming the singly occupied molecular orbital (SOMO) of $Cr(CO)_4(bpy)^{\cdot-}$. The plot of the b_2 SOMO of $Cr(CO)_4(bpy)^{\cdot-}$, depicted in Fig. 4, and the fragment contributions (Table 4) clearly show that the SOMO is composed mainly of the first antibonding π^* MO of the bpy ligand. The contribution from the Cr atom decreases from 2.52 to 1.94% on going from the neutral complex to the anion. The SOMO is partially delocalised onto the CO ligands of the $Cr(CO)_4$ moiety, the contribution from the axial CO ligands being almost twice as large as that from the equatorial ones (Table 4). The mechanisms of SOMO delocalisation on the axial and equatorial CO ligands are, however, very different. The SOMO plot (Fig. 4) demonstrates that the equatorial CO ligands lie in the SOMO nodal plane. Hence, they participate in the SOMO only by their $\pi^*(p_z)$ orbitals, 0.79% each. Analogously, the $\pi^*(p_x)$ orbital of each axial CO ligand participates by 0.54%. More interestingly, the calculations show that the σ-orbital of each axial CO ligand is admixed to the SOMO by 0.86%. Specifically, it is the $\sigma_1 - \sigma_2$ out-of-phase combination of the lone electron pairs of the two axial CO ligands which contributes to the SOMO by 1.72% (*i.e.* 0.86% per axial CO). The axial Cr $4p_z$ orbital contributes very little, by 0.078% only.

Spin densities and EPR spectra

The calculated distribution of total spin density in $Cr(CO)_4(bpy)^{\cdot-}$ is shown in Fig. 5 and summarised in Table 5, which also compares the effect of the basis set on the calculated spin densities and Fermi contact terms. Although there are quantitative differences, the choice of the basis set does not affect the qualitative conclusions outlined below. The calculated total spin density on C atoms of the axial and equatorial CO ligands is about the same, while the contributions due to the unpaired electron in the SOMO differ significantly: 1.16% on each axial C atom and 0.43% one each equatorial one (Table 4). Fig. 5

Table 5 Experimental EPR hyperfine splitting constants (hfs) and calculated isotropic Fermi contact couplings ($10^{-4}\,cm^{-1}$) using different basis sets

Experiment		Basis set I		Basis set II		Basis set III	
Atom	hfs	Fermi contact term	Spin density	Fermi contact term	Spin density	Fermi contact term	Spin density
^{53}Cr	1.197	0.677	−0.0142	0.853	−0.0402	0.682	−0.0096
^{14}N	3.469	4.065	0.1557	3.387	0.1373	2.520	0.1662
$^{1}H^{3,3'}$	0.982	1.590	−0.0040	−1.164	−0.0045	−1.310	−0.0032
$^{1}H^{4,4'}$	1.159	1.090	0.0031	0.792	0.0022	−0.823	−0.0025
$^{1}H^{5,5'}$	4.216	−4.975	−0.0139	−4.503	−0.0136	−4.731	−0.0138
$^{1}H^{6,6'}$	0.701	0.732	0.0020	0.405	0.0015	−1.318	−0.0031
$^{13}C_{ax}$	5.619	4.926	0.0078	5.760	0.0136	5.627	0.0066
$^{13}C_{eq}$	—	0.252	0.0070	0.557	0.0123	0.037	0.0063
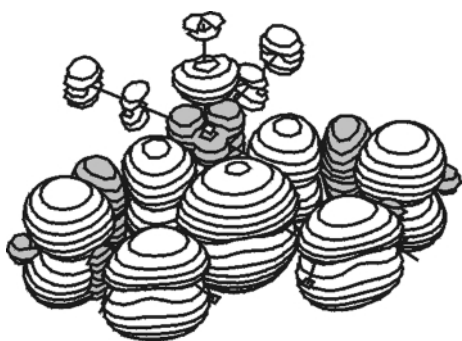
Fig. 5 The spin density distribution in $Cr(CO)_4(bpy)^{\cdot-}$.

also demonstrates that the spin density drops to zero in the horizontal (x,y) symmetry plane of the molecule. On the other hand, a large part of the spin density on the axial C atoms is oriented along the z axis, *i.e.* the axial C–Cr–C σ-bond.

Calculated Fermi contact terms, which amount to the theoretical values of isotropic EPR hyperfine splitting constants, compare well with the experimental values (Table 5). Notably, the experimental EPR spectra of ^{13}CO-enriched $Cr(CO)_4(bpy)^{\cdot-}$ revealed only splitting from the two axial ^{13}C atoms, splitting from the equatorial ones being too small to be resolved. Indeed, the calculated Fermi contact term is much larger for the axial $^{13}C(CO)$ atom than for its equatorial counterpart, despite nearly identical values of the total spin density.

Discussion

In agreement with all available experimental data, our DFT calculations picture the reduction of $Cr(CO)_4(bpy)$ as predominantly bpy-localised but strongly affecting the bonding within the $Cr(CO)_4$ fragment. Specifically, it was calculated that the bpy ligand accommodates *ca.* 76% of the extra electron density in $Cr(CO)_4(bpy)^{\cdot-}$. The unpaired electron is localised on the bpy ligand to an extent of 94%, in the b_2 SOMO which is, essentially, a π*(bpy) orbital. The calculated bond length changes within the Cr(bpy) fragment reflect the respective π bonding and antibonding properties of the b_2 SOMO. It follows that $Cr(CO)_4(bpy)^{\cdot-}$ can be formally viewed as a d^6 chromium(0) complex, with a radical anionic ligand bpy$^{\cdot-}$. Accordingly, experimental UV–VIS absorption[3,6,25,26] and EPR[9] spectra of $Cr(CO)_4(bpy)^{\cdot-}$ resemble closely those of bpy$^{\cdot-}$, being only slightly perturbed by interaction with the $Cr(CO)_4$ moiety.

The remaining 24% of the extra electron density in $Cr(CO)_4(bpy)^{\cdot-}$ resides on the CO ligands. The charge on the Cr atom is almost the same in the neutral and anionic complexes. Reduction involves addition of an electron to the b_2 LUMO of $Cr(CO)_4(bpy)$. This redox orbital becomes singly occupied (SOMO) in the $Cr(CO)_4(bpy)^{\cdot-}$ radical anion, without any significant change in composition. The SOMO is localised on the bpy and the four CO ligands from *ca.* 94

and 4%, respectively. Comparison between the charge and SOMO distribution reveals that the electronic effects of $Cr(CO)_4(bpy)$ reduction are much more delocalised than the SOMO of the radical anion. Namely, the electron density in lower-lying occupied orbitals is redistributed toward the CO ligands, apparently compensating for increased electron donation from the bpy$^{\cdot-}$ ligand. The two equatorial CO ligands accept much more (14.2%) of the extra electron density in the radical anion than the axial CO ligands, which accommodate 9.6%. This computational finding accounts well for the experimentally observed changes of the CO stretching force constants which decrease upon reduction by 68 and 21 N m^{-1} for the equatorial and axial CO ligands, respectively.[9,10] This weakening of the equatorial and, to a lesser extent, axial C≡O bonds is manifested also by calculated elongations of C–O bonds, accompanied by shortenings of Cr–CO bonds, on going from the neutral species to the radical anion (Table 1). These structural effects are much larger for the equatorial Cr–CO units than for the axial ones. The π back bonding to the equatorial CO ligands is stronger than to the axial ones in both the neutral and anionic forms of $Cr(CO)_4(bpy)$.

Mixing between an occupied σ-non-bonding orbital of the axial OC–Cr–CO fragment with the π*(bpy) orbital in the b_2 LUMO and SOMO of $Cr(CO)_4(bpy)$ and its radical anion, respectively, is another interesting feature emerging from the DFT calculations. Its contribution is about the same, *ca.* 1.7%, in both the neutral and anionic complexes. This σ–π* interaction explains straightforwardly the huge difference in the EPR hyperfine splitting from ^{13}C nuclei of axial and equatorial CO ligands. Table 5 shows that the isotropic EPR hyperfine splitting constant is much larger for the axial than equatorial $^{13}C(CO)$ nuclei despite nearly identical spin densities calculated at both positions. This is caused by the fact that the isotropic EPR splitting constants are determined by corresponding Fermi contact terms,[27–29] that is by the spin density at the $^{13}C(CO)$ nuclei due to electrons in s orbitals. Relatively large observed[9] hyperfine splitting, 6.1 G, from axial ^{13}C nuclei originates in the axial σ–π* interaction which mixes the axial C 2s orbital into the SOMO, giving rise to a substantial Fermi contact. On the other hand, no hyperfine splitting was observed from the equatorial $^{13}C(CO)$ nuclei since they lie in the SOMO nodal plane, without any direct s-orbital participation. Hyperfine splitting from equatorial ^{13}C atoms could arise only from a spin polarisation of C 1s and 2s electrons by the unpaired electron density in the C 2p π* orbital. Data in Table 5 clearly show that such a spin polarisation produces Fermi contact term values which are 10–150 times smaller than those of the axial ^{13}C atoms for which the σ–π* mechanism is available. The above analysis of the EPR hyperfine splitting from the $^{13}C(CO)$ nuclei points to two conclusions: (i) the EPR hyperfine splitting from the ^{13}C donor atoms of the CO ligands in $Cr(CO)_4(bpy)^{\cdot-}$ ligand reflects the extent of σ–π* delocalisation, instead of the total spin-density distribution, and (ii) the direct admixture of the C 2s orbital into the SOMO by σ–π* delocalisation contributes toward the isotropic $^{13}C(CO)$ hyperfine splitting constant

at least 10 times more than the spin polarisation of the C 1s and 2s electrons by the unpaired electron density in the C 2p π^* orbital. These conclusions may be extended to the whole family of transition metal complexes with a radical-anionic ligand which often show large EPR hfs from the nuclei of donor atoms in the *cis*-position.[30–34] This effect was traditionally attributed to a 'σ–π hyperconjugation', a term that is often used in a qualitative sense but seldom analysed in detail and explained in terms of specific orbital interactions.[28–32,35]

Similar σ–π^* interaction was recently found to occur in α-diimine complexes containing axial ligands which are bound to the metal atom by high-lying σ-orbitals, *e.g.* metal fragments or alkyls.[36–39] The complexes $Ru(SnPh_3)_2(CO)_2(\alpha$-diimine) or $PtMe_4(\alpha$-diimine) are typical examples. The extent of the σ–π^* interaction in these complexes is, however, much greater than in $Cr(CO)_4(bpy)^{0/\cdot-}$, ranging from 14 to 27%. It appears to be the most important factor determining the ground state structural, spectroscopic and electrochemical properties, as well as the reactivity, emission and lifetimes of the excited states of dinuclear or alkyl complexes with an α-diimine ligand in a *cis* position. Because of its much smaller extent in the $Cr(CO)_4$-$(bpy)^{0/\cdot-}$ complexes studied herein, the σ–π^* interaction does not have such dramatic consequences. Nevertheless, its presence is clearly manifested experimentally by the large EPR hyperfine splitting from the axial $^{13}C(CO)$ atoms.

Parallels are often drawn between MLCT excited states and reduced forms of low-valent metal complexes with reducible ligands.[16] Namely, the resemblance of the spectroscopic (UV–VIS, IR, Raman) properties of an excited molecule to those of electrochemically generated reduced form are deemed diagnostic for the MLCT character of the excited state in question. Indeed, the calculations reported above show that the spectroscopically[6] and photochemically[3,4,11] important '$d_{xz} \rightarrow \pi^*(bpy)$' MLCT excitation increases the electron density at the bpy ligand to the same extent as reduction, by 79 and 76%, respectively. It follows that the charge transfer in the MLCT state is incomplete, partly compensated for by an opposite drift in the electron density distribution.[40] Contrary to a conventional view, the 'hole' created by excitation is delocalised over the whole $Cr(CO)_4$ fragment, instead of being confined to the Cr atom. In fact, the electron density on the Cr atom decreases by 0.36, less than on the four CO ligands which are depopulated, on the total, by 0.426 e$^-$. Axial CO ligands are depopulated *ca.* 1.6 times more than their equatorial counterparts. This computational result agrees with the conclusions based on the Raman spectra measured in resonance with the lowest allowed MLCT transition.[10] The selective enhancement of the Raman band due to the in-phase totally symmetric CO stretching vibrations implies that the axial C≡O bonds are elongated upon the MLCT excitation 1.2–3.0 times more than the equatorial ones. This effect has been ascribed to the depopulation of the Cr d_{xz} orbital which diminishes the π-back bonding to the axial CO ligands more than to the equatorial ones. Moreover, the observed strong intensity enhancement of Raman bands due to the bpy vibrations and deformation vibrations of the Cr(bpy) chelate ring agrees well with the calculated charge redistribution between the Cr atom and bpy ligand.

Conclusions

The DFT calculations on $Cr(CO)_4(bpy)$ and its radical anion reproduce well the experimentally observed spectroscopic effects of $Cr(CO)_4(bpy)$ reduction and enable us to explain them on a structural and electronic basis. The reduction is predominantly localised on the bpy ligand, its structural and electronic effects spreading over the $Cr(CO)_4$ moiety, mostly the CO ligands.

The structural changes of the Cr(bpy) fragment and principal features displayed by electronic absorption and EPR spectra of $Cr(CO)_4(bpy)^{\cdot-}$ are mostly accounted for by the properties of the b_2 SOMO, which is 94% $\pi^*(bpy)$ in character. The $Cr(CO)_4(bpy)^{\cdot-}$ thus spectroscopically behaves as containing a bpy$^{\cdot-}$ ligand.

Analysis of the SOMO alone is insufficient to describe changes in the overall charge distribution in $Cr(CO)_4(bpy)$ upon its reduction. Electronic effects of the reduction are much more delocalised than the SOMO. In particular, the bpy-localised reduction is accompanied by an electron density redistribution toward the equatorial and, to a lesser extent, axial CO ligands. This conclusion explains the experimental observation that the equatorial CO stretching force constant decreases on reduction three times more than the equatorial one.

Two principal mechanisms are responsible for the spin density delocalisation to the CO ligands: (i) a direct participation of $\pi^*(CO)$ orbitals of both equatorial and axial CO ligands in the SOMO, and (ii) an admixture of axial $\sigma(CO)$ orbitals to the SOMO. The latter mechanism operates only for axial CO ligands. It amounts to a σ–π^* interaction between an orbital that has a σ character with respect to the axial OC–Cr–CO bond and the $\pi^*(bpy)$ orbital. It provides the mechanism for a selective increase of spin density in the 1s and 2s orbitals of the axial C atoms. This is experimentally manifested by the isotropic $^{13}C(CO)$ EPR hyperfine splitting constants which are relatively large for the axial $^{13}C(CO)$ but unobservable for the equatorial ones.

The virtual contradiction between the IR and EPR spectroelectrochemical results[9] was resolved: the IR data, *i.e.* the changes in the CO stretching force constants on reduction, reflect the absolute changes of the total electron density on the CO ligands, which are much larger in the equatorial than axial positions. On the other hand, isotropic ^{13}C EPR hyperfine splitting constants of the CO ligands in $Cr(CO)_4(bpy)^{\cdot-}$ do not reflect the total spin densities at respective ^{13}C nuclei but the mechanism of the spin delocalisation, namely the extent of the σ–π^* interaction. Obviously, the isotropic hyperfine splitting constants need not to be a good measure of the total spin density distribution over the donor atoms of 'spectator' ligands in $Cr(CO)_4(bpy)^{\cdot-}$ and analogous complexes with a radical anionic ligand.[30,31,33,34]

The amount of the extra electron density localised on the bpy ligand in a MLCT excited state of $Cr(CO)_4(bpy)$ is about the same as in $Cr(CO)_4(bpy)^{\cdot-}$, underlying the spectroscopic analogy between MLCT and reduced states of complexes containing reducible ligands. MLCT excitation was found to diminish the electron density on the axial and, to a lesser extent, equatorial CO ligands. Obviously, the, so called MLCT excitation, concerns the whole $Cr(CO)_4(bpy)$ molecule and not only the Cr(bpy) fragment, as is usually assumed.

The results and conclusions discussed above can easily be extended to other coordination and organometallic complexes of low-valent metals which contain a reducible or radical-anionic ligand.

Acknowledgements

References

1 D. J. Stufkens, *Coord. Chem. Rev.*, 1990, **104**, 39.
2 R. W. Balk, T. Snoeck, D. J. Stufkens and A. Oskam, *Inorg. Chem.*, 1980, **19**, 3015.
3 J. Víchová, F. Hartl and A. Vlček, Jr., *J. Am. Chem. Soc.*, 1992, **114**, 10903.

4 A. Vlček, Jr., J. Víchová and F. Hartl, *Coord. Chem. Rev.*, 1994, **132**, 167.
5 I. G. Virrels, M. W. George, J. J. Turner, J. Peters and A. Vlček, Jr., *Organometallics*, 1996, **15**, 4089.
6 D. Guillaumont, C. Daniel and A. Vlček, Jr., *Inorg. Chem.*, 1997, **36**, 1684.
7 I. R. Farrell, P. Matousek and A. Vlček, Jr., *J. Am. Chem. Soc.*, 1999, **121**, 5296.
8 D. Miholova and A. A. Vlček, *J. Organomet. Chem.*, 1985, **279**, 317.
9 A. Vlček, Jr., F. Baumann, W. Kaim, F.-W. Grevels and F. Hartl, *J. Chem. Soc., Dalton Trans.*, 1998, 215.
10 A. Vlček, Jr., F.-W. Grevels, T. L. Snoeck and D. J. Stufkens, *Inorg. Chim. Acta*, 1998, **278**, 83.
11 D. Guillaumont, C. Daniel and A. Vlček, Jr., manuscript in preparation.
12 S. Wieland, K. B. Reddy and R. van Eldik, *Organometallics*, 1990, **9**, 1802.
13 W.-F. Fu and R. van Eldik, *Inorg. Chem.*, 1998, **37**, 1044.
14 W. F. Fu and R. van Eldik, *Inorg. Chim. Acta*, 1996, **251**, 341.
15 H. Kobayashi, Y. Kaizu, H. Kimura, H. Matsuzawa and H. Adachi, *Mol. Phys.*, 1988, **64**, 1009.
16 A. Vlček, Jr., *Chemtracts–Inorg. Chem.*, 1993, **5**, 1.
17 M. J. Frisch, G. W. Trucks, H. B. Schlegel, G. E. Scuseria, M. A. Robb, J. R. Cheeseman, V. G. Zakrzewski, J. A. Montgomery, Jr., R. E. Stratmann, J. C. Burant, S. Dapprich, J. M. Millam, A. D. Daniels, K. N. Kudin, M. C. Strain, O. Farkas, J. Tomasi, V. Barone, M. Cossi, R. Cammi, B. Mennucci, C. Pomelli, C. Adamo, S. Clifford, J. Ochterski, G. A. Petersson, P. Y. Ayala, Q. Cui, K. Morokuma, D. K. Malick, A. D. Rabuck, K. Raghavachari, J. B. Foresman, J. Cioslowski, J. V. Ortiz, B. B. Stefanov, G. Liu, A. Liashenko, P. Piskorz, I. Komaromi, R. Gomperts, R. L. Martin, D. J. Fox, T. Keith, M. A. Al-Laham, C. Y. Peng, A. Nanayakkara, C. Gonzalez, M. Challacombe, P. M. W. Gill, B. Johnson, W. Chen, M. W. Wong, J. L. Andres, C. Gonzalez, M. Head-Gordon, E. S. Replogle and J. A. Pople, Gaussian 98, Revision A.6, Gaussian, Inc., Pittsburgh, PA, 1998.
18 K. Andersson, M. R. A. Blomberg, M. P. Flüscher, G. Karström, V. Kellö, R. Lindh, P.-Å. Malmqvist, J. Noga, J. Olsen, B. O. Roos, A. J. Sadlej, P. E. M. Siegbahn, M. Urban and P.-O. Widmark, MOLCAS version 3.0, University of Lund, Sweden, 1994.
19 A. D. Becke, *J. Chem. Phys.*, 1993, **98**, 5648.
20 N. Godbout, D. R. Salahub, J. Andzelm and E. Wimmer, *Can. J. Chem.*, 1992, **70**, 560.
21 T. H. Dunnning and P. J. Hay, in *Modern Theoretical Chemistry*, ed. H. F. Schaefer, III, Plenum, New York, 1976.
22 C. Adamo and V. Barone, *Chem. Phys. Lett.*, 1997, **274**, 242.
23 W. J. Hehre, R. Ditchfield and J. A. Pople, *J. Chem. Phys.*, 1972, **56**, 2257.
24 T. Clark, J. Chandrasekhar and P. v. R. Schleyer, *J. Comput. Chem.*, 1983, **4**, 294.
25 H. Saito, J. Fujita and K. Saito, *Bull. Chem. Soc. Jpn.*, 1968, **41**, 863.
26 H. Saito, J. Fujita and K. Saito, *Bull. Chem. Soc. Jpn.*, 1968, **41**, 359.
27 B. A. Goodman and J. B. Raynor, *Adv. Inorg. Chem. Radiochem.*, 1970, **13**, 135.
28 M. Symons, *Chemical and Biochemical Aspects of Electron-Spin Resonance Spectroscopy*, Van Nostrand Reinhold Company Ltd., Wokingham, England, 1978.
29 J. E. Wertz and J. R. Bolton, *Electron Spin Resonance. Elementary Theory and Practical Applications*, Chapman and Hall, New York, 1986.
30 W. Kaim, *Coord. Chem. Rev.*, 1987, **76**, 187.
31 W. Kaim and S. Kohlmann, *Inorg. Chem.*, 1990, **29**, 2909.
32 W. Kaim, *Inorg. Chem.*, 1984, **23**, 3365.
33 A. Klein, C. Vogler and W. Kaim, *Organometallics*, 1996, **15**, 236.
34 F. Hartl and A. Vlček, Jr., *Inorg. Chem.*, 1996, **35**, 1257.
35 W. Kaim, B. Olbrich-Deussner, R. Gross, S. Ernst, S. Kohlmann and C. Bessenbacher, in *Importance of Paramagnetic Organometallic Species in Activation, Selectivity and Catalysis*, eds. M. Chanon, M. Julliard and J.-C. Poite, Kluwer Academic Publishers, Dordrecht, The Netherlands, 1989.
36 M. P. Aarnts, D. J. Stufkens, M. P. Wilms, E. J. Baerends, A. Vlček, Jr., I. P. Clark, M. W. George and J. J. Turner, *Chem. Eur. J.*, 1996, **2**, 1556.
37 M. P. Aarnts, M. P. Wilms, K. Peelen, J. Fraanje, K. Goubitz, F. Hartl, D. J. Stufkens, E. J. Baerends and A. Vlček, Jr., *Inorg. Chem.*, 1996, **35**, 5468.
38 W. Kaim, A. Klein, S. Hasenzahl, H. Stoll, S. Záliš and J. Fiedler, *Organometallics*, 1998, **17**, 237.
39 S. Hasenzahl, H.-D. Hausen and W. Kaim, *Chem. Eur. J.*, 1995, **1**, 95.
40 B. S. Brunschwig, C. Creutz and N. Sutin, *Coord. Chem. Rev.*, 1998, **177**, 61.

Paper 9/03560E